EFFECT OF ARTIFICIAL AGEING ON THE DEFECT SUSCEPTIBILITY OF TENSILE PROPERTIES TO POROSITY VARIATION IN A356 ALUMINIUM ALLOYS

Choong Do Lee

Department of Metallurgical and Materials Engineering, Inha Technical College, Nam-gu, Incheon, Republic of Korea

Abstract

The present study aims to estimate the dependence of the tensile properties on microporosity variation in low-pressure die-cast A356 aluminium alloys with respect to various T6 treatment conditions and to investigate the relative contribution of the strain-hardening exponent and damage evolution of eutectic Si particles in terms of the defect susceptibility of the tensile properties to effective void area fraction. The solution treatment was performed for 3, 6 and 12 h at 540 °C, and the artificial ageing was conducted for 4, 16 and 48 h at 140–180 °C. The defect susceptibility of the tensile properties to microporosity variation depends practically upon the ageing time, whereas the solutionising time has a minor effect on the variability in the defect susceptibility. Additionally, the maximum value of the ultimate tensile strength (UTS) achievable in a defect-free condition remarkably increases with the ageing treatment, and it also slightly increases with the solutionising time.

The maximum value of the tensile elongation for a defect-free condition depends practically upon the solutionising time, even though it generally decreases with ageing treatment. The main reason that the UTS and elongation exhibit different responses with regard to the solutionising and ageing treatments is the variation in the strain-hardening exponents associated with the T6 treatment. The frequency of the damage evolution of eutectic Si particles by the cracking mode is considerably decreased with the ageing treatment, and this transition under ageing treatment has additional contributions to the variation in the defect susceptibility of tensile properties to effective void area fraction.

Keywords: tensile property, A356 aluminium alloy, microporosity, defect susceptibility

Introduction

The existence of micro-voids plays a significant role in determining the mechanical properties of a casting and is considered as a decisive factor that restricts wide-ranging applications of heavy duty parts in the structural components, and many experimental and theoretical works have recently been conducted on the effect of internal discontinuities on the mechanical properties of Al–Si alloys.[1–14] Typically, Cáceres et al.[1,2] reported that the UTS and elongation of Al–Si alloys depends on porosity variations via theoretical predictions derived from experimental results. Additionally, Gokhale and his colleagues[3–7] suggested that the tensile elongation of Al–Si alloys is empirically described in terms of a power law relationship between the defect susceptibility of the tensile elongation to microporosity variation and a maximum value achievable in a defect-free condition, as described in Eqn. 1:

$$\varepsilon_i = \varepsilon_h [1 - f]^a \qquad \text{Eqn. 1}$$

where ε_i is the tensile elongation of a material with a microporosity f, ε_h is the maximum tensile elongation of a defect-free material, and a is defined as the defect susceptibility of the tensile elongation to microporosity variations. Similarly, it is reported that the UTS can also be described with a power law dependence on the microporosity variation, as described in Eqn. 2:[9,10]

$$\sigma_i = \sigma_h [1 - f]^b \qquad \text{Eqn. 2}$$

where σ_i is the UTS of a material with a microporosity f, σ_h is the maximum value of the UTS achievable in a defect-free material, and b is the defect susceptibility of the UTS to microporosity variation. However, despite the many studies in this research field,[3–5,8–10,14] the physical meaning of defect susceptibility in the empirical relationships shown in Eqns. 1 and 2 has not been clearly described in terms of

the theoretical validity on constitutive laws of tensile deformation.

On the other hand, it is well known that the mechanical properties of heat-treatable aluminium alloys vary markedly on the solution treatment and artificial ageing conditions during the T6 treatment.[15] Our previous study on the defect susceptibility of the tensile strength to microporosity variation proposed the optimal T6 treatment conditions in terms of the effective void area fraction, which is composed of the area fraction of pre-existing micro-voids and the additional change of the area fraction by the damage evolution of eutectic Si particles.[14] Based on this, the variations in the defect susceptibility of the tensile properties after a T6 treatment are simultaneously related to the age hardening on the T6 treatment as well as the existence of internal discontinuities, such as the micro-cracks formed by the damage evolution of eutectic Si particles and the pre-existing micro-voids formed by the casting process.

Nevertheless, the relative contributions of the hardening ability brought on by the artificial ageing and the existence of internal discontinuities to the overall tensile properties of T6-treated alloys have not been determined. Furthermore, the dependence of the tensile properties on the solution and ageing processes used in the T6 treatment is not still defined in terms of the variation of strain-related factors, such as the strain-hardening exponent and the strain rate sensitivity.

Therefore, as a sequential study on previous study,[14] this study aims to estimate the variability in the defect susceptibility of the tensile properties to variations in the effective void area fraction during the T6 treatment, through the systematic estimation of the strain rate sensitivity and strain-hardening exponent on the T6 treatment. Additionally, it also aims to evaluate the relative contribution of transition mode on the damage evolution of eutectic Si particles by age hardening to the effective void area fraction using the constitutive model.

Experimental Procedure

Specimen Preparation

The raw material used in this study was commercial grade A356 alloy, and its typical chemical composition is listed in Table 1. The test specimens were prepared via a low-pressure die-casting process in the form of an automobile wheel (5 spokes, 18 inch diameter) and from a position of the spoke section. And, the test specimens were prepared via various T6 treatment conditions (solution treatment; 3, 6 and 12 h at 540 °C, artificial ageing; 4, 16 and 48 h at 140, 160 and 180 °C).[14]

Tensile Test and Measurement of the Microporosity

The tensile specimens were prepared to plate-type specifications with 30 mm gauge length and 6 mm gauge width. The tensile test was carried out at room temperature under strain rate conditions of 2.78×10^{-4} s^{-1} using an extensometer. The UTS, yield strength (YS), and tensile elongation (elongation to fracture) were chosen as the typical tensile properties, and the nominal value of YS was measured as the stress level at 0.2% offset strain. The strain rate sensitivity (SRS) was measured at room temperature using the incremental strain rate change method.[16] In the strain rate change test, the initial strain rate was 2.78×10^{-4} s^{-1}, and a second strain rate of 2.78×10^{-3} s^{-1} was applied at an engineering strain of 2.0%. The strain-hardening exponent (SHE) was measured by plotting of the stress–strain curve on a log–log scale for a strain range corresponding to obvious plastic deformation.

The microporosity was measured through quantitative fractography by scanning electron microscope (SEM) observations on the fractured surfaces of the entire test specimens, and its nominal value was expressed in terms of the area ratio of the micro-voids to the entire area of the fracture surface.

Experimental Results

Microstructural Characteristics

Figure 1 shows typical micrographs of the as-cast and T6-treated A356 alloys. The area fraction of eutectic Si particles remarkably decreases as the solutionising time increases, and the individual sizes of eutectic Si particles and the spacings between the Si particles in the eutectic Si colonies depend practically upon the solutionising time; a remarkable spheroidisation of eutectic Si particles is also seen with increasing solutionising time.

Typical values of the microstructural characteristics of the T6-treated alloys are listed in Table 2. The area fraction of eutectic Si particles decreases from 15.4% in the as-cast condition to 10.6% in the T6-treated alloy with 12-h

Table 1. Chemical Composition of the A356 Aluminium Alloy

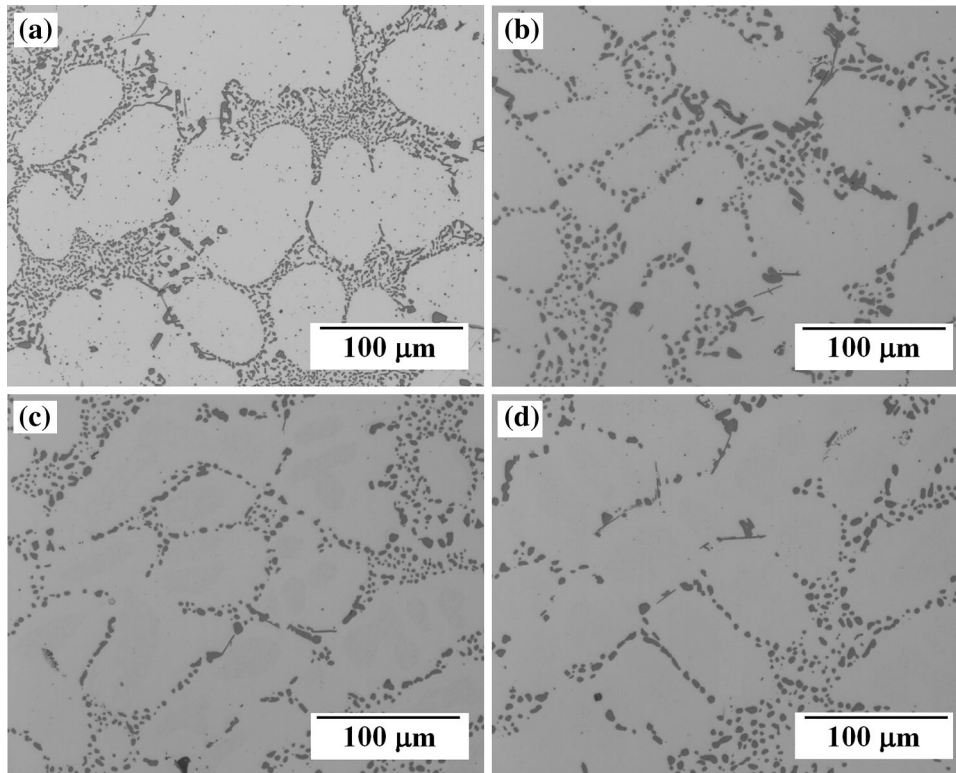| Elements	Si	Mg	Mn	Cu	Fe	Ti	Sr	Al
Composition (wt%)	7.18	0.35	0.01	0.14	0.02	0.14	0.02	Bal.

Figure 1. Microstructural views of the as-cast and T6-treated A356 alloys: (a) as-cast, (b) 3 h-, (c) 6 h- and (c) 12-h solutionised conditions.

Table 2. Variation of the Microstructural Features in the A356 Alloy from the Solution Treatment[14]

Condition	As-cast alloy	Solutionising time (with artificial ageing at 160 °C/16 h)		
		3 h	6 h	12 h
Microstructural features				
Area fraction of eutectic Si particles (%)	15.4	11.6	11.4	10.6
SDAS (μm)	60.2	61.5	62.6	64.1
Spacing between Si particles in colony (μm)	1.8	2.9	3.8	5.2
Average diameter of individual Si particles (μm)	1.6	2.8	3.3	4.5

Table 3. Variation in the Area Fractions of Eutectic Si Particles by the Artificial Ageing Treatment for a 6-h Solutionised Alloy

Condition	Solutionised, only	Artificially aged at 160 °C		
		4 h	16 h	48 h
Microstructural features				
Area fraction of eutectic Si particles (%)	12.4	11.8	11.4	9.1

area fraction of eutectic Si particles gradually decreases as the ageing time increases, even though its nominal value is not noticeably decreased during the initial ageing stage.

Tensile Properties

Figure 2 shows typical values describing the dependence of the tensile properties on the solutionising time with regard to the lapse of ageing time. As shown, the overall levels of UTS and YS gradually increase with the solutionising time. These results indicate that the increases in the UTS and YS as a result of the hardening effect from the ageing treatment are approximately 80 and 120 MPa, respectively, even though they exhibit slightly different aspects with the solutionising time. However, the nominal value of the tensile elongation practically decreases from a range of
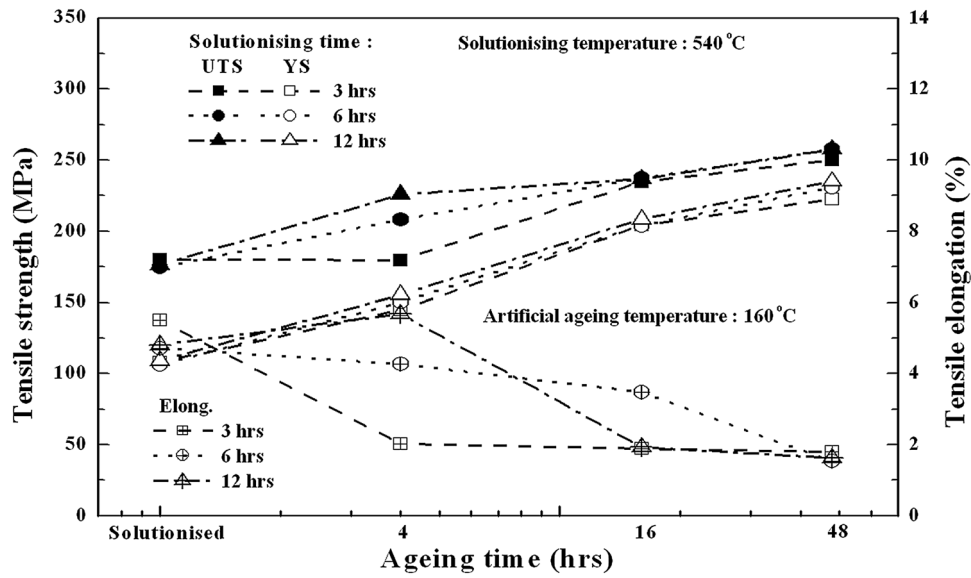
solutionised condition. Additionally, the secondary dendrite arm spacing (SDAS) and the spacing between Si particles in the eutectic Si colonies increase from 60.2 and 1.8 μm of as-cast condition to 64.1 and 5.2 μm of 12 h solution treatment, respectively.

As a typical example of the microstructural change from artificial ageing, the variation in the area fraction of eutectic Si particles for different ageing times on a 6-h solutionised alloy is listed in Table 3. This shows that the

Figure 2. Variability in the tensile properties for different solutionising conditions with ageing time.
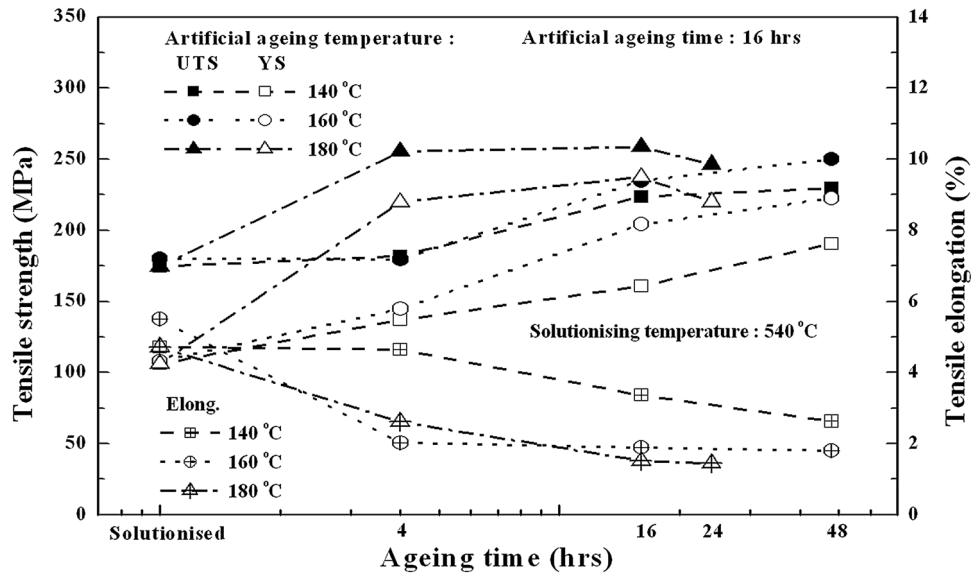

Figure 3. Overall tensile properties with respect to ageing time for different ageing temperatures.

4–6% for the solutionised condition to approximately 2% as the ageing treatment proceeds.

Figure 3 shows the overall trend in the tensile properties with regard to variations in the ageing time for different ageing temperatures. The nominal levels of the UTS and YS increase with the ageing temperature, and the optimal ageing time to a peak-ageing condition is shortened as the ageing temperature increases. Conversely, the tensile elongation is remarkably decreased as the ageing temperature increases, even though the tensile elongation of specimens aged at 140 °C exhibits a gradually decreasing trend compared to that of specimens aged at other temperatures.

Figure 4 shows the variability in the nominal value of the strain-hardening exponent for each solutionising and ageing condition. As shown in Figure 4a, the strain-hardening exponents of the T6-treated specimens are practically influenced by the ageing treatment, rather than the solution treatment, i.e., the nominal value of the exponent is decreased from approximately 0.14–0.08 as the ageing temperature increases from 140 to 180 °C. Figure 4b exhibits that the overall dependence of strain-hardening exponent on the ageing condition, i.e., the nominal value of strain-hardening exponent decreases from 0.19 to a range of 0.08–0.12 as the ageing time increases, even though there is a small deviation. Additionally, note that the
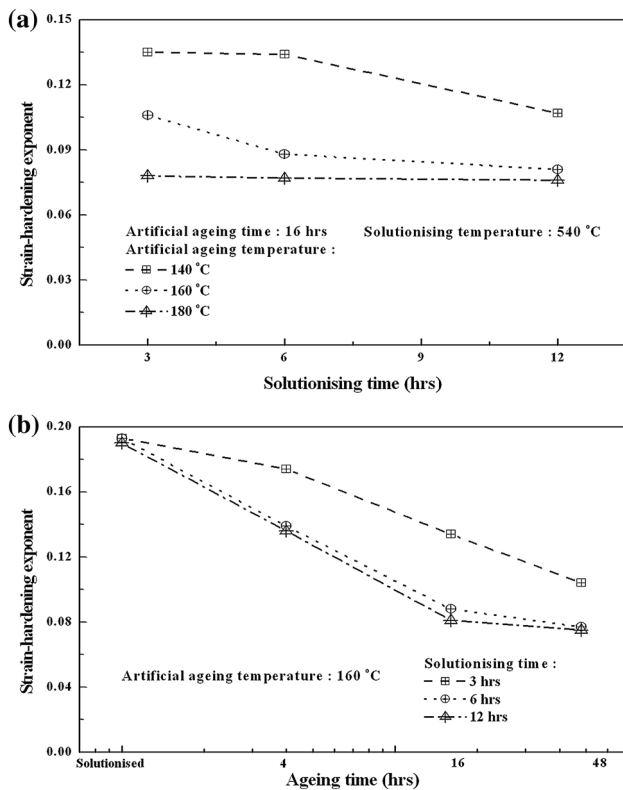
Figure 4. Variation in strain-hardening exponents with respect to (a) solutionising time and (b) ageing time for different T6 treatment conditions.

decreasing trend for the strain-hardening exponent becomes more sensitive with the solutionising time.

On the other hand, the strain rate sensitivity of A356 alloy is not practically influenced by T6 treatment, and typical values of the strain rate sensitivity are listed in Table 4. As listed in Table 4, the nominal value of the strain rate sensitivity is not sensitive to the solutionising time but only slightly depends on whether the specimen was artificially aged or only solutionised, i.e. the average value of the strain rate sensitivity wholly decreases from approximately 0.013 for the solutionised condition to 0.010 for the T6-treated condition with an ageing treatment of 16 h at 160 °C.

Typical SEM images of the fracture surface of the T6-treated alloys are shown in Figure 5. The fracture surface is

Table 4. Variation in the Strain Rate Sensitivity of the A356 Alloy with Solution Treatment

Solutionising time	3 h	6 h	12 h
Alloy condition			
Solutionised only	0.013	0.012	0.012
Aged during 16 h at 160 °C	0.010	0.010	0.010

composed of the fracture regions of mixed phase between the Al matrix and eutectic Si colony, with pre-existing micro-voids which are randomly distributed over the entire fracture surface. As shown, the fracture morphology of both alloys is very similar, with the exception of the fracture morphology of eutectic Si colony in the 12-h solutionised alloy that is slightly rougher than that of eutectic Si colony in the 3-h solutionised alloy, due to the coarsening of individual Si particles by the increase of solutionising time.

Defect Susceptibility of Tensile Properties on T6 Treatment

Figure 6 shows the variability in the defect susceptibilities of the UTS and tensile elongation to microporosity variation for the various T6 treatment conditions. As shown, the overall dependence of the tensile properties on the microporosity variation can be described as a linear relationship in terms of the logarithmic function between the tensile properties and microporosity variation, i.e. the defect susceptibility. The linear slope of the UTS on the microporosity variation becomes more or less insensitive as the ageing time increases, whereas the tensile elongation exhibits a more sensitive dependence to the ageing time. Additionally, the nominal value of the defect susceptibility and the maximum value can be described, as shown in Figures 7, 8, based on the variations in the solutionising and ageing conditions.

As shown in Figure 7, the defect susceptibility of the UTS clearly decreases from that of the solutionising condition as the ageing time increases, and its nominal level of initial ageing stage and solutionised condition is also slightly decreased with increases in the solutionising time. The maximum value of the UTS achievable in a defect-free condition increases from approximately 200 MPa for a solutionising condition to a range of 260–280 MPa for an ageing time of 48 h. Additionally, the maximum value of the UTS for a defect-free condition also practically increases with the solutionising time.

However, in the case of the tensile elongation shown in Figure 8, the defect susceptibility remarkably increases with the ageing treatment, with a slight deviation from an overall trend. It can note that the defect susceptibility of tensile elongation depends more clearly upon the lapse of ageing time, compared with the defect susceptibility of the UTS. The maximum value of the tensile elongation clearly decreases as the ageing time increases, even though the overall level exhibits an obvious dependence on the solutionising condition. Additionally, it indicates that the maximum value of the tensile elongation in the 12-h solutionised condition is not practically affected by variations in the ageing time, nor is the maximum value for the 48 h-aged condition.
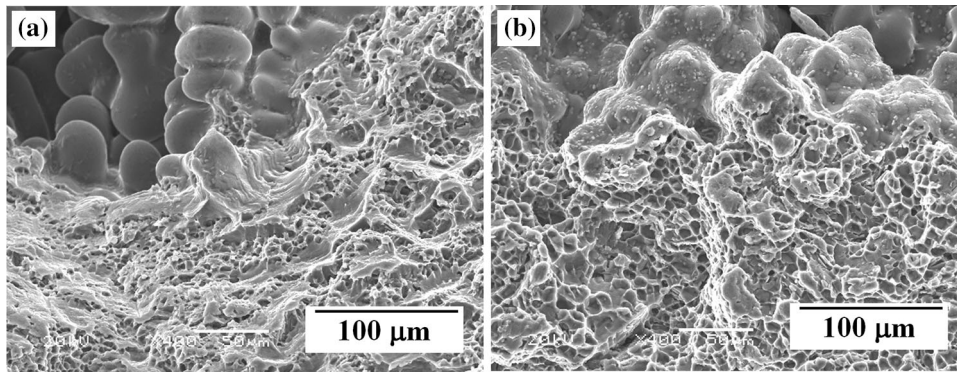
Figure 5. SEM views of the fracture morphology for different T6-treated alloys: (a) 3-h and (b) 12-h solutionised alloys with 16 h-ageing at 160 °C.
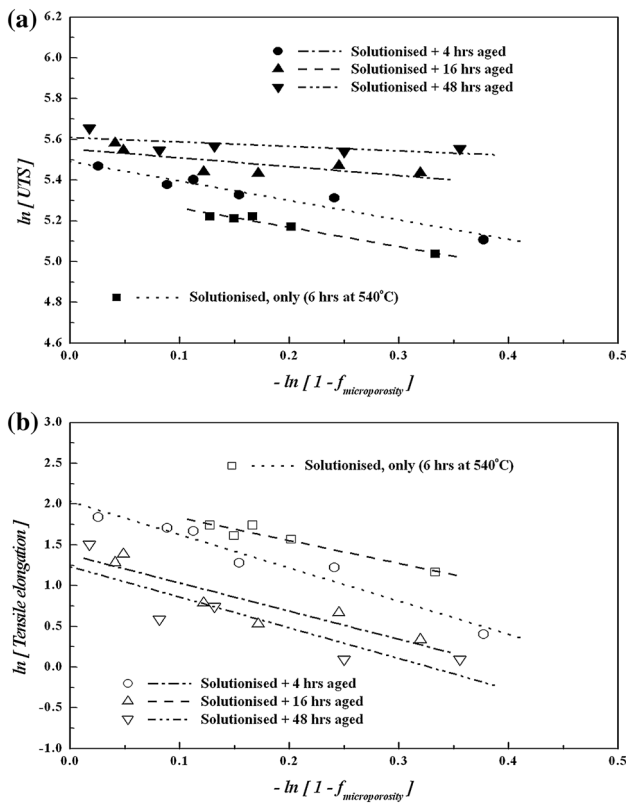

Figure 6. Dependence of the tensile properties on the microporosity variation for T6-treated alloys with a solution treatment of 6 h at 540 °C and ageing at 160 °C: (a) UTS and (b) elongation.
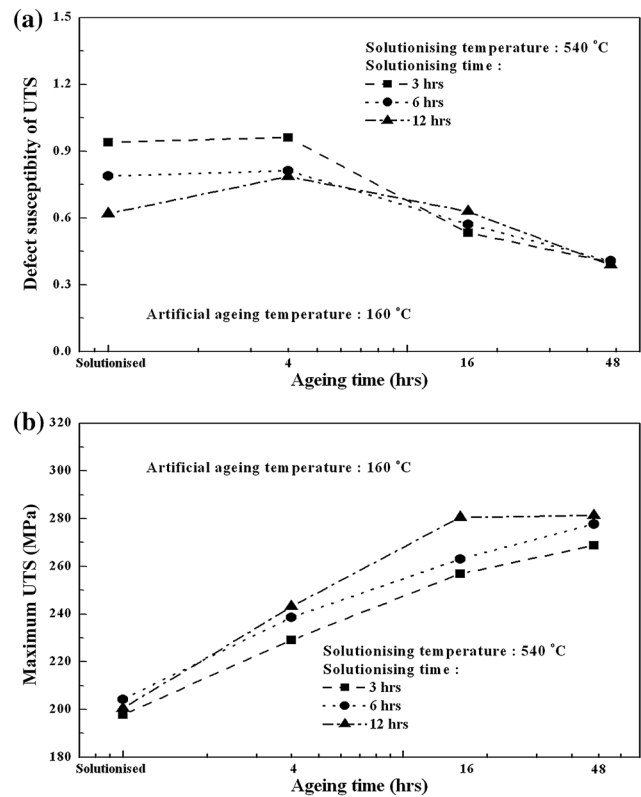

Figure 7. Variations in the (a) defect susceptibility and (b) maximum value for a defect-free condition of the UTS with respect to ageing time for different solutionising conditions.

Discussion

Strain-Hardening Exponent on Defect Susceptibility

Assuming a material containing a micro-void is plastically deformed with axial local equilibrium under tensile conditions, the stress distribution inside a material using the power law relation ($\sigma = K\varepsilon^n \dot{\varepsilon}^m$) can be described by Eqn. 3:[17,18]

$$\sigma_i(1-f)A_0 e^{-\varepsilon i} = \sigma_h A_0 e^{-\varepsilon h} \qquad \text{Eqn. 3}$$

where σ_i, ε_i and σ_h, ε_h are the true stress and true strain in the near and far fields from the void region, respectively. And, n and m are the strain-hardening exponent and strain rate sensitivity, respectively, and their numerical expression are $(\partial \ln \sigma / \partial \ln \varepsilon)_{\dot{\varepsilon}, T}$ and $(\partial \ln \varepsilon / \partial \ln \dot{\varepsilon})_{\varepsilon, T}$, respectively. Additionally, given that A_0 is the initial cross-sectional area of a material and f is the area fraction of pre-existing micro-void, $A_0(1-f)$ describes the actual load-carrying capacity inside the material.
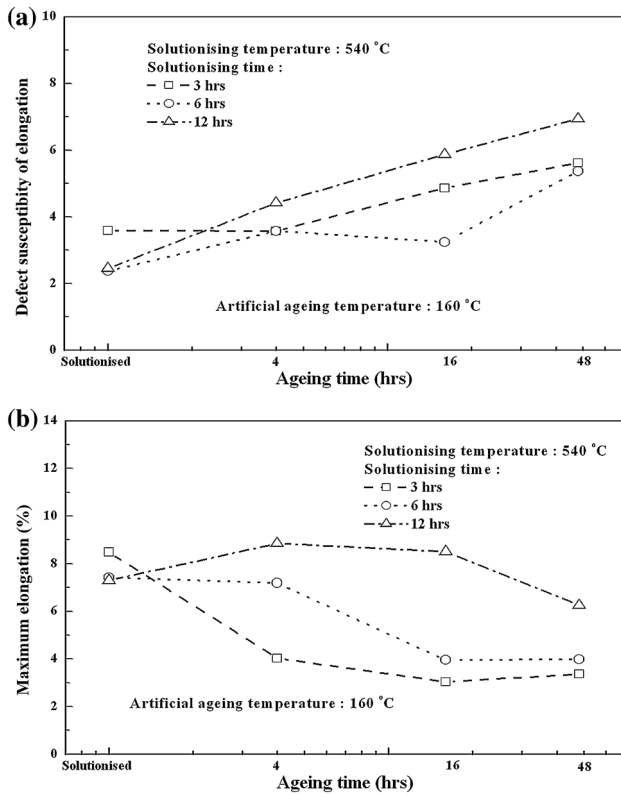
Figure 8. Variation in the (a) defect susceptibility and (b) maximum value for a defect-free condition of the tensile elongation with respect to ageing time for different solutionising conditions.
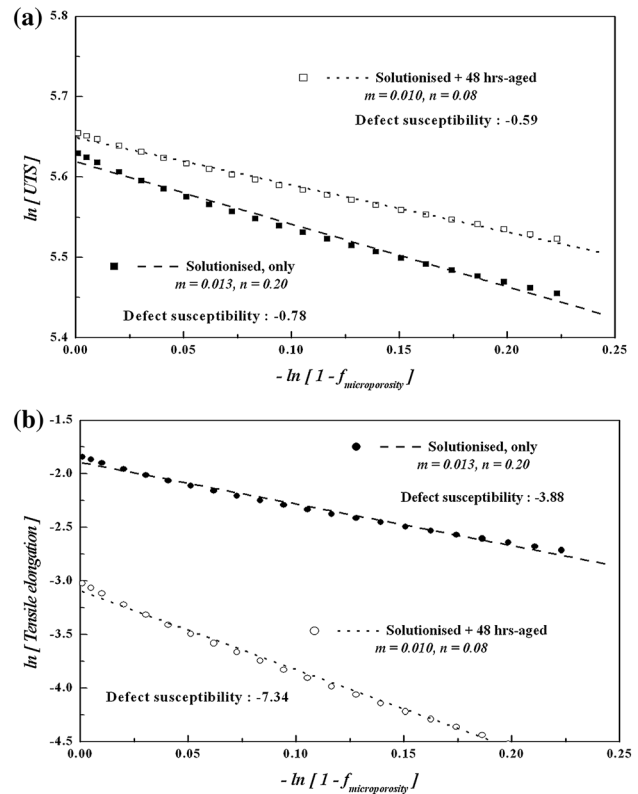
Figure 9. Theoretical predictions from the modified constitutive model for the defect susceptibility of the tensile properties to microporosity variations in the solutionised and T6-treated conditions.

The theoretical estimation for the relative increment of near and far field strains on the microporosity variation can be achieved using constitutive models for tensile instability as following equation.[17,18]

$$\Delta\varepsilon_h = \left((1-f)(b/b_0)(c/c_0)e^{\varepsilon i} \right)^{1/m} e^{-\varepsilon i/m} \Delta\varepsilon_i$$
$$\left[(\Delta\varepsilon_i/m)n(\varepsilon_i^{n/m-1}) - (\Delta\varepsilon_i/m)(\varepsilon_i^{n/m}) + \varepsilon_i^{n/m} \right] \Big/ \left[e^{-\varepsilon h/m} \varepsilon_h^{n/m} \right]$$

Eqn. 4

where $\Delta\varepsilon_i$ and $\Delta\varepsilon_h$ are the relative increasement of near and far field strains, respectively, and the (b/b_0) and (c/c_0) terms correspond to the Rice-Tracey equation for lateral void growth.

Figure 9 shows a typical example of the theoretical prediction for variations in the defect susceptibility of the tensile properties to microporosity variations using the modified constitutive model.[18] The defect susceptibility of the UTS slightly decreases with the decrease of the strain-hardening exponent by artificial ageing after solution treatment, whereas the defect susceptibility of the tensile elongation in the T6-treated condition is considerably increased. Additionally, the maximum value of the UTS achievable in a defect-free condition is practically increased via the decrease in the strain-hardening exponent as a result of the T6 treatment, but the maximum value of the tensile elongation is drastically decreased by the

variations in the strain-hardening exponent. This approach exhibits good agreement with the experimental results shown in Figures 7 and 8.

Additionally, the dependence of defect susceptibility on the variation of strain-hardening exponent can be directly described by substituting the empirical equations for the defect susceptibility [Eqns. 1 and 2] into the power law relation for tensile deformation. Assuming that the strain rate sensitivity in the near and far fields from the void region is same, the defect susceptibility of the tensile elongation to microporosity variation, *a*, can be proposed by substituting Eqn. 1 into the power law relation, as shown in Eqn. 5.

$$a = -(1/n)\{(\varepsilon_h - \varepsilon_i) + \ln(1-f)\}/\ln(1-f)$$

Eqn. 5

Likewise, the defect susceptibility of the UTS to microporosity variation, *b*, can be described using Eqn. 6, with the expansion of the numerical formula for the empirical relationship of the defect susceptibility of the UTS shown in Eqn. 2.

$$b = \{-(\varepsilon_h - \varepsilon_i)/\ln(1-f) + 1\}$$

Eqn. 6

Equations 5 and 6 indicate that the defect susceptibility of the tensile properties is fundamentally related to the strain-

hardening exponent and the difference between the near and far field strains in the void region.

Damage Evolution of Si Particles on the Defect Susceptibility

Figure 10 shows the cross-sectional views of the fractured specimens in the solutionised and T6-treated conditions. A trace of damage evolution of eutectic Si particles in the cracking mode for the T6-treated condition is restricted to the near field region of the fracture surface as the ageing treatment proceeds (Figure 10b, c), whereas the damage
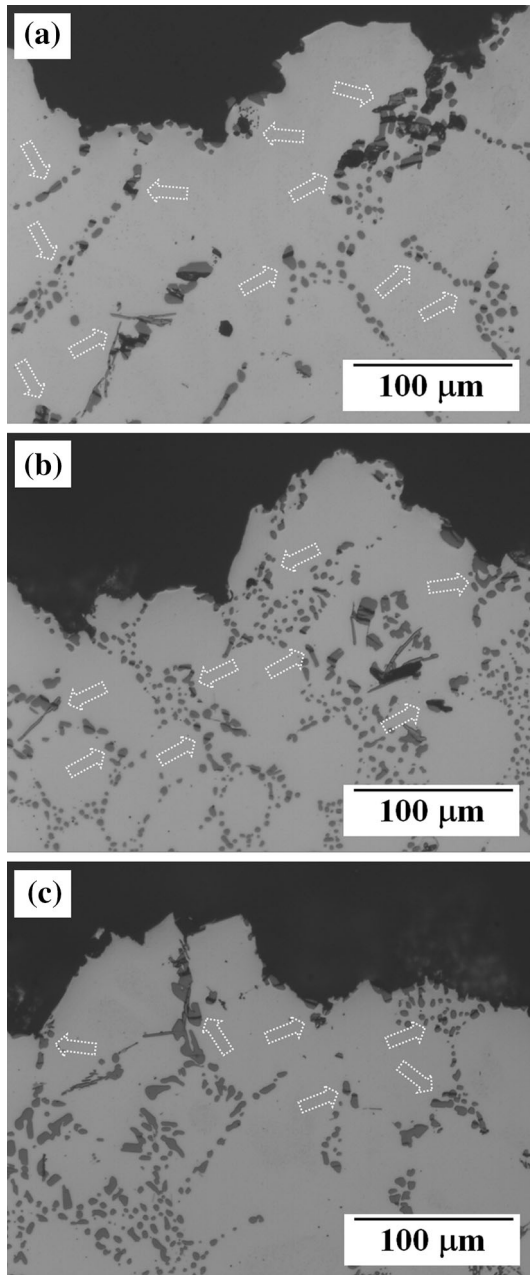

Figure 10. Cross-sectional views of the damage evolution of eutectic Si particles near to the fracture surface of T6-treated alloys: (a) solutionised alloy, (b) 16 h-aged and (c) 48 h-aged alloys at 160 °C.

evolution of eutectic Si particles in the solutionised condition is widely distributed over the far field region from the fracture surface (Figure 10a).

Furthermore, it can be noted that the frequency of damage evolution from the eutectic Si particles is also remarkably decreased as the ageing time increases after the solutionising treatment. The main reason for this is that the strengthening effect of the α-Al matrix region by the formation of fine Mg_2Si precipitate on artificial ageing restricts a further plastic deformation to α-Al matrix,[15] and finally, this induces an obvious reduction on the nominal width of localised region near to the fracture surface, accompanying the damage evolution of eutectic Si particles.

For the damage evolution of eutectic Si particles in an Al–Si alloy, Poole et al.[19] reported that the damage evolution of Si particles is focused at an initial stage of plastic deformation, which is approximately 1–3%. Additionally, a practical description for the damage evolution of a brittle 2nd phase, such as the eutectic Si particles, can be provided in terms of the incoherency parameter proposed in the modified constitutive model, as following Eqn. 7:[18]

$$\eta = \left(\varepsilon_i - \varepsilon_f^*\right)\big/\varepsilon_i \qquad \text{Eqn. 7}$$

where ε_f^* is the fracture strain for the localised damage evolution of eutectic Si particles, and ε_i is the macroscopic fracture strain of a material containing internal discontinuities.

From this, the incoherency parameter eventually decreases via the decrease of the macroscopic fracture strain ε_i by strengthening effect of α-Al matrix region, even though the fracture strain for the damage evolution of eutectic Si particles ε_f^* is not practically influenced by the ageing treatment. Therefore, the nominal level of the coherency parameter for the damage evolution of eutectic Si particles decreases with the ageing treatment, and the relative contribution of the damage evolution of eutectic Si particles to the effective void area fraction inside a material decreases practically with the ageing treatment.

Therefore, the relative contributions of the damage evolution of eutectic Si particles and the microporosity variations to the effective void area fraction can be expressed as shown in Eqn. 8.[18]

$$f = \eta_{\text{void}} f_{\text{void}}\big/P(\alpha)_{\text{void}} + \eta_{\text{Si}} f_{\text{Si}}\big/P(\alpha)_{\text{Si}} \qquad \text{Eqn. 8}$$

where η_{void} and f_{void} are the incoherency parameter and the area fraction of the pre-existing micro-voids, respectively, and η_{Si} and f_{Si} are the incoherency parameter and the area fraction of eutectic Si particles, respectively. Additionally, $P(\alpha)_{\text{void}}$ and $P(\alpha)_{\text{Si}}$ are the plastic constraint factors for internal discontinuities, which describe the size distribution and geometric configuration of the pre-existing micro-

voids and fractured Si particles inside a material, which are described by the numerical formula $P(\alpha) = \left[\alpha(n) \middle/ (a/l)^2 + 1.24 \middle/ (b(b+l))^{0.5} \right]$, where a and b are size descriptions of the internal discontinuities, and l is the size of a ligament between the internal discontinuities. The numerical expression of $\alpha(n)$ is $0.1 + 0.217n + 4.83n^2$, where n is the strain-hardening exponent.[20,21]

Figure 11 shows the predicted results for the overall dependence of the tensile properties to microporosity variations with regard to different combination of the incoherency parameter and strain-hardening exponent, in terms of the effective void area fraction as shown in Eqn. 8. For simplicity, it is assumed that the nominal value of the strain-hardening exponent decreases from 0.2 for the solutionised condition to 0.1 as the ageing treatment proceeds, whereas the incoherency parameter for the damage evolution of eutectic Si particles decreases from 1.0 for the solutionised condition to 0.1 for the fully aged condition.

As shown, the theoretical prediction exhibits a very similar trend as the experimental results as shown in Figures 7 and 8, i.e., the defect susceptibility of the tensile elongation to microporosity variations is remarkably increased, whereas the defect susceptibility of the UTS is slightly decreased as a result of the ageing treatment. This indicates that the tensile properties of a material simultaneously containing the pre-existing micro-voids and brittle 2nd phase particles depend fundamentally upon the variability in the effective void area fraction and strain-relating factors. Additionally, the overall dependence of tensile properties on T6 treatment as well as as-cast condition can practically describe via the theoretical prediction by modified constitutive model which is consisted of the effective void area fraction-terms such as the microporosity, incoherency parameter and plastic constraint factor, and the strain-relating factors such as the strain-hardening exponent and strain rate sensitivity.[18]

Summary

1. The defect susceptibility of the UTS to microporosity variation decreases, whereas the defect susceptibility of the tensile elongation increases with the ageing time. The solutionising time has a minor effect on the variability of defect susceptibility on the tensile properties. Additionally, the maximum value of the UTS achievable in a defect-free condition is noticeably increased with the ageing treatment and slightly increased with the solutionising time. The maximum value of tensile elongation can be improved by increasing the solutionising time, even though it depends practically upon the ageing treatment.

2. The main reason that the UTS and tensile elongation exhibit different responses with regard to the solutionising and ageing treatments is due to the variations in the strain-hardening exponent as a result of the T6 treatment. Additionally, the strengthening effect of artificial ageing treatment induces the decrease of strain-hardening exponent, and this is directly related to the variability in the defect susceptibility of tensile properties to microporosity variation. The strain rate sensitivity has no practical effect on the variation of the defect susceptibility because the strain rate sensitivity of aged alloys exhibits not only a low level but also is not practically changed as the ageing time increases.

3. The transition of the damage evolution of eutectic Si particles with the ageing treatment also contributes to the variability in the defect susceptibility of tensile properties, in terms of the effective void area fraction. The frequency of the damage evolution of eutectic Si particles is considerably decreased with strengthening effect of α-Al matrix region as the ageing treatment proceeds, and this induces a practical variation in the effective void area fraction, which decides the load-carrying capacity inside a material containing pre-existing micro-voids.
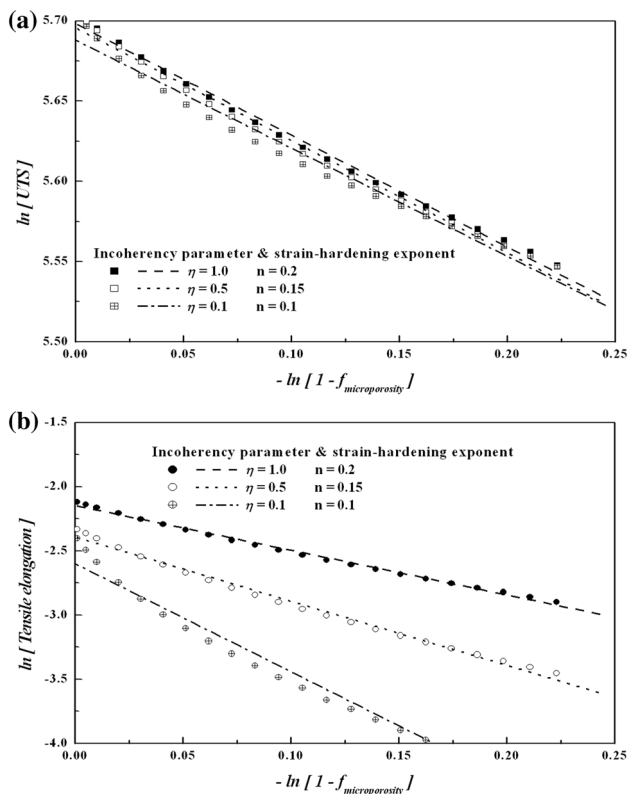
Figure 11. *Variability in the defect susceptibility of the tensile properties to microporosity variations predicted using the modified constitutive model for different incoherency parameters and strain-hardening exponents.*

Acknowledgements

REFERENCES

1. C.H. Cáceres, Scr. Metall. **32**, 1851–1855 (1995)
2. C.H. Cáceres, B.I. Selling, Mater. Sci. Eng. A **220**, 109–116 (1996)
3. A.M. Gokhale, G.R. Patel, Mater. Charact. **54**, 13–20 (2005)
4. A.M. Gokhale, G.R. Patel, Mater. Sci. Eng. A **392**, 184–190 (2005)
5. A.M. Gokhale, G.R. Patel, Scr. Mater. **52**, 237–241 (2005)
6. M.F. Horstemeyer, A.M. Gokhale, Int. J. solids struct. **36**, 5029–5055 (1999)
7. M.F. Horstemeyer, J. Lathrop, A.M. Gokhale, M.D. Dighe, Theor. appl. fract. mech. **33**, 31–47 (2000)
8. M.D. Dighe, A.M. Gokhale, Scr. Mater. **37**, 1435–1440 (1997)
9. C.D. Lee, Mater. Sci. Eng. A **488**, 296–302 (2008)
10. C.D. Lee, Mater. Sci. Eng. A **527**(3144), 3144–3150 (2010)
11. J.P. Bandstra, D.A. Koss, Mater. Sci. Eng. A **319–321**, 490–495 (2008)
12. G. Huber, Y. Brechet, T. Pardoen, Acta Mater. **53**, 2739–2749 (2005)
13. J. Gammage, D. Wilkinson, Y. Brechet, D. Embury, Acta Mater. **52**, 5255–5263 (2004)
14. T.I. So, W.C. Jung, C.D. Lee, K.S. Shin, Met. Mater. Int. **21**, 842–849 (2015)
15. J.E. Hatch, *Aluminum—Properties and Physical Metallurgy* (ASM, Ohio, 1984)
16. G.E. Dieter, *Mechanical Metallurgy*, 3rd edn. (McGraw-Hill, New York, 1986)
17. A.K. Ghosh, Acta Metall. **25**, 1413–1424 (1977)
18. C.D. Lee, K.S. Shin, Y.J. Kim, Eng Mater Frac. **175**, 339–356 (2017)
19. W.J. Poole, N. Charra, Mater. Sci. Eng. A **406**, 300–308 (2005)
20. A. Weck, D.S. Wilkinson, Acta Mater. **56**, 1774–1784 (2008)
21. T. Pardoen, J.W. Hutchinson, J. Mech. Phys. Solids **48**, 2467–2512 (2000)